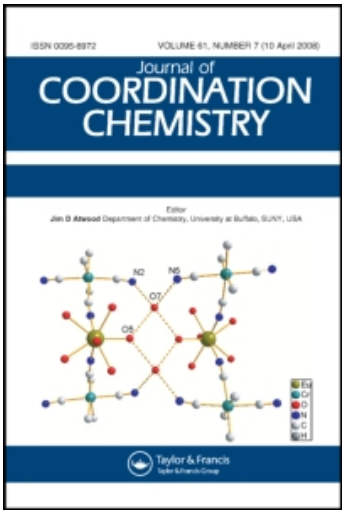

Journal of Coordination Chemistry
Publication details, including instructions for authors and subscription information:
http://www.informaworld.com/smpp/title~content=t713455674

Divalent metal complexes of an amide-appended N_3O-donor ligand: synthesis, structural and spectroscopic features, and amide methanolysis reactivity

Gajendrasingh K. Ingle[a]; Rex W. Watkins[a]; Atta M. Arif[b]; Lisa M. Berreau[a]
[a] Department of Chemistry & Biochemistry, Utah State University, Logan, UT 84322-0300 [b] Department of Chemistry, University of Utah, Salt Lake City, UT 84112

To cite this Article Ingle, Gajendrasingh K. , Watkins, Rex W. , Arif, Atta M. and Berreau, Lisa M.(2008) 'Divalent metal complexes of an amide-appended N_3O-donor ligand: synthesis, structural and spectroscopic features, and amide methanolysis reactivity', Journal of Coordination Chemistry, 61: 1, 61 — 77
To link to this Article: DOI: 10.1080/00958970701731974
URL: http://dx.doi.org/10.1080/00958970701731974

Journal of Coordination Chemistry
Vol. 61, No. 1, 10 January 2008, 61–77

Divalent metal complexes of an amide-appended N_3O-donor ligand: synthesis, structural and spectroscopic features, and amide methanolysis reactivity§

GAJENDRASINGH K. INGLE†, REX W. WATKINS†, ATTA M. ARIF‡ and LISA M. BERREAU*†

†Department of Chemistry & Biochemistry, Utah State University, 0300 Old Main Hill, Logan, UT 84322-0300
‡Department of Chemistry, University of Utah, Salt Lake City, UT 84112

(*Received 23 June 2007; in final form 27 July 2007*)

Divalent zinc, cobalt, and nickel complexes of an amide-appended N_3O-donor ligand (mpppa, *N*-methyl-*N*-((6-pivaloylamido-2-pyridyl)methyl)-*N*-(2-pyridylethyl)amine) have been prepared and characterized. X-ray crystallographic studies indicate that $[(mpppa)Zn(CH_3CN)](ClO_4)_2$ (**1**) exhibits a distorted square pyramidal geometry, whereas $[(mpppa)M(CH_3OH)(H_2O)](ClO_4)_2$ (M = Co (**2**·**H₂O**), Ni (**3**)) exhibit distorted octahedral structures. Each complex was also characterized by analytical and spectroscopic methods. Treatment of **1** with $Me_4NOH \cdot 5H_2O$ in methanol-containing solutions results in amide methanolysis. This reaction proceeds via the initial formation of a deprotonated amide intermediate, $[(mpppa^-)Zn]ClO_4$ (**4**), which has been isolated and characterized. Kinetic studies performed as a function of the amount of methanol present revealed saturation behavior with respect to the alcohol concentration. Variable temperature kinetic studies yielded activation parameters ($\Delta H^{\ddagger} = 19.8$ kcal/mol; $\Delta S^{\ddagger} = -3.8(1)$ eu) that are interestingly different from those exhibited by a zinc complex of an amide-appended N_4O-donor ligand. These results are discussed in the context of the overall coordination number and geometry of the zinc center. Treatment of **2** and **3** with $Me_4NOH \cdot 5H_2O$ in methanol-containing solutions does not result in amide methanolysis.

Keywords: Zinc; Amide; Methanolysis; Cobalt; Nickel

1. Introduction

The coordination chemistry of chelate ligands containing amide appendages is an area of interest with regard to the design of new biomimetic systems and catalysts. For example, a tris(2-pyridylmethyl)amine ligand containing a single amide appendage (ppbpa, *N*-((6-pivaloylamido)-2-pyridyl)methyl)-*N*,*N*-bis((2-pyridyl)methyl)amine, Figure 1) has been used to construct synthetic complexes of biological relevance (e.g. (μ-peroxo)dicopper(II) complexes [1]) and in the development of new ruthenium oxidation catalysts [2,3]. We, and others, have examined the coordination and amide

*Corresponding author. Email: berreau@cc.usu.edu
§Contribution for Peter Williams issue.

ISSN 0095-8972 print/ISSN 1029-0389 online © 2008 Taylor & Francis
DOI: 10.1080/00958970701731974

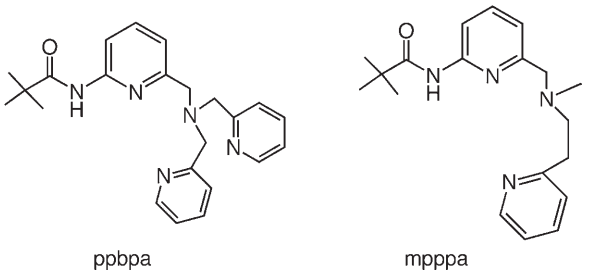

Figure 1. Drawings of the ppbpa and mpppa ligands.

cleavage chemistry of zinc complexes of this ligand [4–9]. Mechanistic studies have revealed that these amide hydrolysis/methanolysis reactions proceed via the initial formation of a deprotonated amide intermediate that subsequently reacts with HOR ($R = H$ or $-CH_3$) to yield the reactive zinc species for intramolecular amide cleavage [4,5]. During the course of our studies, we became interested in evaluating how the overall coordination number of the chelate ligand and the nature of the metal ion influence amide cleavage reactivity. In the work outlined herein we describe the preparation and amide methanolysis reactivity of a zinc complex of a N_3O(amide)-donor ligand (mpppa, *N*-methyl-*N*-((6-pivaloylamido-2-pyridyl)methyl)-*N*-(2-pyridylethyl)amine, figure 1) [10]. We have also investigated the chemistry of Co(II) and Ni(II) complexes of the mpppa ligand and found that such complexes do not exhibit amide cleavage reactivity.

2. Experimental

2.1. *Chemicals and reagents*

All reagents were obtained from commercial sources and were used as received. The ligand *N*-methyl-*N*-((6-pivaloylamido-2-pyridyl)methyl)-*N*-(2-pyridylethyl)amine (mpppa) was prepared as previously described [10].

CAUTION! Perchlorate salts of organic ligands are potentially explosive. These should always be handled carefully and in small amounts [11].

2.2. *Physical methods*

^1H and $^{13}C\{^1H\}$ NMR spectra of diamagnetic species were collected on a JEOL GSX-270, JEOL ECX-300, or Bruker ARX-400 NMR spectrometer. Chemical shifts are referenced to the residual solvent peak in CD_2HCN (^1H: 1.94 ppm (quintet); ^{13}C: 1.39 ppm (heptet)). FTIR spectra were recorded on a Shimadzu FTIR-8400 spectrometer. Elemental analyses were performed by Atlantic Microlab, Inc., Norcross, GA. Mass spectrometry experiments were performed at the University of California, Riverside.

2.3. *Preparation of divalent metal complexes*

2.3.1. [(mpppa)Zn(CH_3CN)](ClO_4)$_2$ (1). A sample of mpppa (80 mg, 0.25 mmol) was dissolved in methanol (~3 mL) and this solution was added to solid $Zn(ClO_4)_2 \cdot 6H_2O$ (92 mg, 0.25 mmol). The resulting mixture was stirred for ~10 min, during which time all of the $Zn(ClO_4)_2 \cdot 6H_2O$ dissolved. The reaction mixture was then separated into three equal portions. Diethyl ether (~20 mL) was added to each portion, producing cloudy solutions. These solutions were placed in a freezer (~−20°C) for 16 h. At this point, the supernatant liquid was decanted, and the remaining white solid was dried under vacuum. Recrystallization via Et_2O diffusion into a $MeOH/CH_3CN$ solution of the complex yielded crystals suitable for X-ray crystallography (0.12 g, 77%). Anal. Calcd. for $C_{21}H_{29}N_5Cl_2O_5Zn$(%): C, 40.08; H, 4.65; N, 11.13. Found: C, 39.92; H, 4.59; N, 10.93. ^{1}H NMR (CD_3OD, 270 MHz) δ 8.96 (d, $J = 5.2$ Hz, 1 H), 8.07–8.23 (m, 2 H), 7.62–7.73 (m, 2 H), 7.56 (d, $J = 8.0$ Hz, 1 H), 7.48 (d, $J = 7.6$ Hz, 1 H), 4.24 (d, $J = 15.2$ Hz, 1 H), 3.95 (d, $J = 15.2$ Hz, 1 H), 3.46 (d, $J = 13$ Hz, 2 H), 3.22 (m, 2 H), 2.51 (s, 3 H), 2.04 (s, 3 H), 1.51 (s, 9H) ppm; $^{13}C\{^1H\}$ NMR (CD_3OD, 67.9 MHz) δ 185.9, 162.1, 153.9, 153.5, 150.1, 144.7, 142.4, 128.4, 125.3, 122.3, 117.0, 63.1, 58.0, 43.7, 42.6, 32.3, 27.5 ppm (17 signals expected and observed); FTIR (KBr, cm^{-1}) 3379 ($\nu_{N\text{-}H}$), 2293 (ν_{CH3CN}), 1660 ($\nu_{C=O}$), 1622, 1100 (ν_{ClO4}), 623 (ν_{ClO4}).

2.3.2. [(mpppa)Co(CH_3OH)](ClO_4)$_2$ (2). A methanol solution (3 mL) of mpppa (0.082 g, 0.25 mmol) was added to solid $Co(ClO_4)_2 \cdot 6H_2O$ (0.092 g, 0.25 mmol). The resulting mixture was stirred for ~30 min at room temperature. The solution was then split in equal volumes into three different glass vials and an excess of Et_2O (~15 mL) was added to each vial. After cooling these solutions at ~ −15°C for two hours the solvent was decanted and the remaining solid was carefully dried under vacuum. Recrystallization of the solid via Et_2O diffusion into a methanol:isopropanol (1 : 1) solution yielded red-pink crystals suitable for single crystal X-ray crystallographic studies (125 mg, 78%). These crystals have an analytical formulation of **2 · H_2O**; the coordinated water molecule is lost upon crushing and drying of the sample: Anal. Calcd. for $C_{20}H_{30}N_4Cl_2O_{10}Co$(%): C, 39.02; H, 4.92; N, 9.11. Found: C, 39.23; H, 4.96; N, 9.02. FTIR (KBr, cm^{-1}) ~3380 (br, $\nu_{N\text{-}H}$), 1662 ($\nu_{C=O}$), 1622, 1091 (ν_{ClO4}), 624 (ν_{ClO4}); UV-vis (CH_3OH), nm (ε, $M^{-1}cm^{-1}$) 500 (20).

2.3.3. [(mpppa)Ni(CH_3OH)(H_2O)](ClO_4)$_2$ (3). Synthesis and recrystallization performed in a manner similar to that described for **2** except using $Ni(ClO_4)_2 \cdot 6H_2O$. Yield: 79% (purple crystals). Anal. Calcd. for $C_{20}H_{32}N_4Cl_2O_{11}Ni$(%): C, 37.97; H, 5.10; N, 8.86. Found: 37.53; H, 4.96; N, 8.92. FTIR (KBr, cm^{-1}) ~3380 (br, $\nu_{N\text{-}H}$), 1662 ($\nu_{C=O}$), 1622, 1091 (ν_{ClO4}), 624 (ν_{ClO4}). UV-vis (CH_3OH), nm (ε, $M^{-1}cm^{-1}$) 578 (7), 850 (16).

2.4. *Amide cleavage reactivity of 1*

2.4.1. Evaluation of the amide cleavage reactivity using ^{1}H NMR. Treatment of **1** (0.038 g, 0.064 mmol) with $Me_4NOH \cdot 5H_2O$ (0.012 g, 0.064 mmol) in CD_3OD (~0.6 mL) resulted in the immediate deposition of a white solid (Me_4NClO_4) in the

NMR tube. Heating of the mixture for 24 h at 45° C resulted in spectral changes consistent with amide methanolysis. Specifically, the *t*-butyl methyl signal shifted to 1.17 ppm and now belongs to a volatile species, as removal of the solvent from the reaction mixture results in the loss of this signal. This product has been previously identified as methyl trimethylacetate in the amide methanolysis reaction of $[(ppbpa)Zn](ClO_4)_2$ [5]. The zinc complex produced in the reaction was not isolated, but instead the chelate ligand of this complex was removed and characterized as outlined below.

2.4.2. Isolation and identification of *N*-((6-amino-2-pyridyl)-*N*-methyl-*N*-(2-pyridylethyl)amine (apmpa) from amide methanolysis of 1. For large-scale ligand recovery experiments of the amide cleavage reaction of **1** a triflate analog of **1** was generated. This complex was prepared by mixing mpppa (0.20 g, 0.61 mmol) and $Zn(OTf)_2$ (0.22 g, 0.61 mmol) in methanol (20 mL) and stirring for 10 minutes at ambient temperature. In independent experiments ^{1}H NMR and FTIR spectra were used to characterize the product of this reaction. The ^{1}H NMR features in CD_3CN are similar to those of **1**, providing evidence for the triflate species in d_3-acetonitrile being $[(mpppa)Zn(CD_3CN)](OTf)_2$ (^{1}H NMR (CD_3CN, 400 MHz) δ 9.69 (br, 1 H), 8.92 (d, $J = 5.2$ Hz, 1 H), 8.10 – 8.02 (m, 2 H), 7.62 (t, $J = 6.7$ Hz, 1 H), 7.50 – 7.44 (m, 2 H), 7.35 (d, $J = 7.6$ Hz, 1 H), 4.30 (d, $J = 15.2$ Hz, 1 H), 3.83 (d, $J = 15.2$ Hz, 1 H), 3.38 – 3.10 (m, 4 H), 2.48 (s, 3 H), 1.44 (s, 9 H) ppm; the 1700–1600 cm^{-1} region of the FTIR spectrum of the triflate analog indicates amide coordination ($\nu_{C=O}$ 1660 cm^{-1}) as found in **1**). To the solution of the triflate analog was added solid $Me_4NOH \cdot 5H_2O$ (0.13 g, 0.68 mmol). This mixture was refluxed under N_2 for 14 h. After cooling the solution to room temperature, aqueous Na_2EDTA (0.36 g, 7.4 mmol) was added and the resulting cloudy mixture was stirred vigorously for ~15 min. The solution was then extracted with CH_2Cl_2 (3 × 30 mL), the combined organic fractions dried over Na_2SO_4, the solution filtered, and the solvent removed from the filtrate under reduced pressure (131 mg, 89%). ^{1}H NMR (CD_3CN, 270 MHz) δ 8.45 (d, $J = 4.9$ Hz, 1 H), 7.70 – 7.57 (m, 1 H), 7.41 – 7.08 (m, 3 H), 6.52 (d, $J = 7.3$ Hz, 1 H), 6.34 (d, $J = 7.3$ Hz, 1 H), 4.74 (br, 2 H), 3.42 (s, 2 H), 3.00 – 2.91 (m, 2 H), 2.85 – 2.74 (m, 2 H), 2.24 (s, 3 H) ppm; ^{13}C{^{1}H} NMR (CD_3CN, 67.9 MHz) δ 161.9, 160.0, 159.0, 150.1, 138.7, 137.1, 124.2, 122.1, 112.9, 107.2, 64.4, 58.3, 42.8, 36.8 ppm (14 signals expected and observed); DEI-MS, *m*/*z* (relative intensity), 242 ($[M]^+$, 3%), HREI-MS, *m*/*z*: calcd for $[C_{14}H_{18}N_4]^+$, 242.1531; found, 242.1531; FTIR (neat, cm^{-1}) 3324 (asymmetric $\nu_{N\text{-}H}$), 3180 (symmetric $\nu_{N\text{-}H}$).

2.4.3. Control reaction: requirement of base for amide methanolysis reactivity. The chelate ligand mpppa (0.054 g, 0.16 mmol) was dissolved in methanol (~10 mL) and this solution was added to solid $Zn(OTf)_2$ (0.058 g, 0.16 mmol). The resulting clear, colorless solution was refluxed under nitrogen for 14 h. Removal of the solvent under reduced pressure and analysis of the residue by ^{1}H NMR in CD_3CN revealed the presence of $[(mpppa)Zn(CD_3CN)](OTf)_2$.

2.4.4. Isolation and characterization of $[(mpppa^-)Zn]ClO_4$ (4). Admixture of mpppa (0.057 g, 0.18 mmol) and $Zn(ClO_4)_2 \cdot 6H_2O$ in acetonitrile (~3 mL), followed by transfer

of this solution to a vessel containing $Me_4NOH \cdot 5H_2O$ (0.035 g, 0.19 mmol) dissolved in methanol, produced a cloudy, colorless solution. This mixture was stirred for ~5 min at which point the solvent was removed under reduced pressure. The remaining precipitate was dissolved in CH_2Cl_2 (~5 mL) and the solution passed was through a celite/glass wool plug. The filtrate was then added to excess hexanes (~20 mL) and cooled to ~ −15°C for ~12 h which resulted in the deposition of a white powder. The solvent was decanted from this solid, which was then carefully dried under vacuum (30 mg, 36%). Anal. Calcd. for $C_{19}H_{25}N_4ClO_5Zn$(%): C, 46.71; H, 5.16; N, 11.48. Found: C, 47.17; H, 5.52; N, 11.24. This complex exhibits concentration and temperature dependent ^{1}H NMR features. All resonances were identified as broad peaks at 0.1 M and 338 K: ^{1}H NMR (CD_3CN, 300 MHz, 0.1 M, 338 K) δ 8.83 (1 H), 7.90 (1 H), 7.67 (1 H), 7.43 – 7.37 (2 H), 7.00 – 6.75 (2 H), 4.00 – 3.50 (2 H), 3.35 – 2.80 (4 H), 2.30 (3 H), 1.22 (9 H) ppm; $^{13}C\{^1H\}$ NMR (CD_3OD, 75.6 MHz, 0.1 M, 338 K) δ 186.2, 161.2, 152.0, 150.9, 142.0 (overlap of two resonances), 127.4, 124.6, 122.7, 119.0, 63.0, 57.0, 45.1, 42.0, 33.6, 29.2 ppm (17 signals expected, 16 identified; one aromatic resonance has not been identified likely due to overlap); FTIR (KBr, cm^{-1}) 1451, 1097 (ν_{ClO4}), 624 (ν_{ClO4}).

2.4.5. Procedure for kinetic studies of the amide methanolysis reaction of 1. Rates of the amide methanolysis reaction of **1** were determined using a procedure previously described for the amide methanolysis reaction of [(ppbpa)Zn]$(ClO_4)_2$ [5]. Data were collected using either a JEOL GSX-270 or JEOL ECX-300 spectrometer. The disappearance of the *t*-butyl methyl signal (1.22 ppm) of [(mpppa$^-$)Zn]ClO_4 (**4**) was monitored and the concentration of this deprotonated amide complex as a function of time was determined using an internal standard ($HCPh_3$). Pseudo first-order rate constants were determined from slopes of plots of ln[**4**] versus time. Data included in these plots represent at least three half-lives of the amide methanolysis reaction. Typical correlation coefficients for these plots were ≥0.998. Using rate data (collected in triplicate) obtained for the temperature range of 42–73° C an Eyring plot was constructed.

2.5. *Evaluation of the reactivity of 2 and 3 with $Me_4NOH \cdot 5H_2O$ in methanol*

The chelate ligand mpppa (0.045 g, 0.14 mmol) was combined with $M(ClO_4)_2 \cdot 6H_2O$ (0.14 mmol; M = Co or Ni) in methanol (~8 mL). This homogeneous mixture was then added to $Me_4NOH \cdot 5H_2O$ (0.15 mmol) dissolved in methanol (~4 mL). For the Co(II) reaction, this addition resulted in a color change from pink to pink/brown, whereas in the Ni(II) reaction a color change from blue to yellow was observed. In each case, the resulting mixture was heated at 50°C for 48 h. At this point, after the reaction mixture was cooled to room temperature, an aqueous solution of $Na_2EDTA \cdot 2H_2O$ (0.42 mmol) was added and the solution was stirred at ambient temperature for 1 h. Adjustment of the pH to ~11, followed by extraction with CH_2Cl_2 (3 × 50 mL), drying of the combined organic fractions over Na_2SO_4, filtration, and removal of the solvent from the filtrate, yielded a yellow brown oil (0.12–0.14 mmol). The ^{1}H NMR spectra of the oils obtained from the Co(II) and Ni(II)-containing reactions indicated the presence of only the unaltered mpppa ligand.

2.6. *X-ray crystallography*

2.6.1. Data collection and refinement. Crystals of **1**, **2** · $\mathbf{H_2O}$ and **3** were each mounted on a glass fiber using a viscous oil and were then transferred to a Nonius KappaCCD diffractometer with MoKα radiation ($\lambda = 0.71073$ Å). The methodology used for determination of final unit cell constants has been previously reported [5]. For the data collected for **1**, **2** · $\mathbf{H_2O}$ and **3** each reflection was indexed, integrated, and corrected for Lorentz, polarization, and absorption effects using DENZO-SMN and SCALEPAC [12]. All non-hydrogen atoms were refined with anisotropic displacement coefficients.

2.6.2. Structure solution. Complex **1** crystallizes in the space group $P2_1/c$. All hydrogen atoms were located and refined independently. Complexes **2** · $\mathbf{H_2O}$ and **3** crystallize in the $P2_12_12_1$ space group. For these complexes, all hydrogen atoms except those on the coordinated methanol molecule were located and refined independently. The methanol hydrogen atoms were assigned isotropic displacement coefficients ($U(\mathrm{H}) = 1.5U(\mathrm{C_{methyl}})$) and their coordinates were allowed to ride on C(20) using SHELXL97 [13]. In **2** · $\mathbf{H_2O}$ and **3** one perchlorate anion exhibits disorder of the chlorine atom and one oxygen atom. In these pseudo octahedral complexes the metal-coordinated methanol molecule participates in a hydrogen bonding interaction with an oxygen atom (O(6)) of the disordered perchlorate anion. The metal-coordinated water molecule in these complexes also participates in hydrogen bonding interactions with the perchlorate anions.

3. Results and discussion

3.1. *Synthesis and characterization of 1–3*

3.1.1. Synthesis. Treatment of the mpppa chelate ligand with equimolar amounts of $M(ClO_4)_2 \cdot 6H_2O$ (M = Zn, Co, Ni), followed by recrystallization, yielded a new series of divalent metal complexes (scheme 1). Each complex was isolated as a crystalline solid in >75% yield and was characterized by elemental analysis, X-ray crystallography, and spectroscopic methods.

3.1.2. Elemental analysis. The elemental analysis data for **1**–**3** are consistent with each complex having at least one coordinated solvent molecule. X-ray crystallographic studies confirmed the analytical formulations and revealed that while the powdered, dried Co(II) complex **2** has only one coordinated methanol molecule, the crystalline form also has a coordinated water molecule.

3.1.3. X-ray crystallography. ORTEP drawings of the cations of **1**, **2** · $\mathbf{H_2O}$ and **3** are shown in figure 2. Details of the X-ray data collection and refinement are given in table 1. Bond distances and angles within these cations are given in table 2. The zinc center in **1** has a coordination number of five and exhibits a distorted-square pyramidal

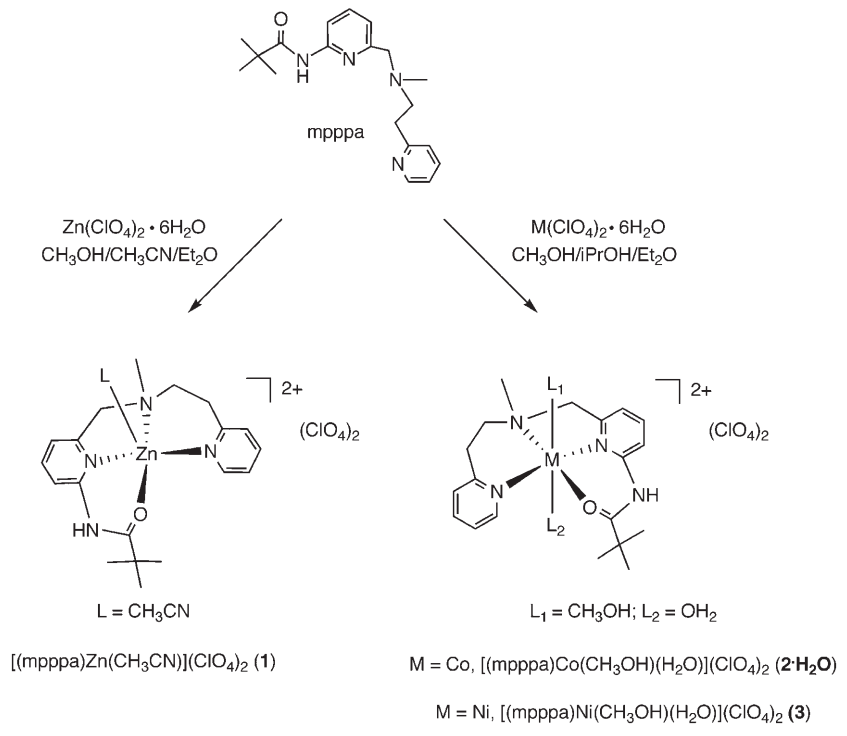

Scheme 1. Synthesis of divalent metal complexes.

geometry ($\tau = 0.30$) [14], with the coordinated acetonitrile in the axial position. The zinc center in $[(ppbpa)Zn](ClO_4)_2$ also has a coordination number of five but has a distorted trigonal bipyramidal geometry ($\tau = 0.77$) [14], with the amide oxygen and tertiary amine nitrogen being in the axial positions [5,8]. The coordinated acetonitrile molecule in **1** binds on the same side of the pseudo square plane to which the N–CH_3 moiety of the chelate ligand is directed. The Zn(1)–O(1) distance in **1** (2.0765(14) Å) is ~0.07 Å longer than the corresponding distance in $[(ppbpa)Zn](ClO_4)_2$ (2.008(3) Å) [5,8]. This suggests a subtle difference in the degree of amide activation in these complexes. However, comparison of the amide C–O and C–N bond distances contradicts this notion, as these distances are identical within experimental error.

Complexes $\mathbf{2 \cdot H_2O}$ and **3** are nearly isostructural, each with a pseudo octahedral metal center. The mpppa is coordinated in a tetradentate manner with the N_3O array of donors in a nearly planar arrangement (O(1)–N(2)–N(3)–N(4) torsion angle: $\mathbf{2 \cdot H_2O}$: −5.4°; **3**: −5.1°). Two trans positions are occupied by water and methanol. In both complexes, methanol coordination occurs on the same side of the pseudo square plane to which the N–CH_3 moiety of the chelate ligand is directed. This suggests that in the dried, bulk sample of **2** wherein the coordinated water molecule is lost, a structure similar to that of **1** may be present. The shortest M–O distance in $\mathbf{2 \cdot H_2O}$ and **3** is for the metal-oxygen amide linkage ($\mathbf{2 \cdot H_2O}$ 2.052(2); **3**: 2.039(2) Å). These distances are slightly shorter than that found in **1**. The amide C–O and C–N bond distances in $\mathbf{2 \cdot H_2O}$ and **3** are identical within experimental error to those of **1**.

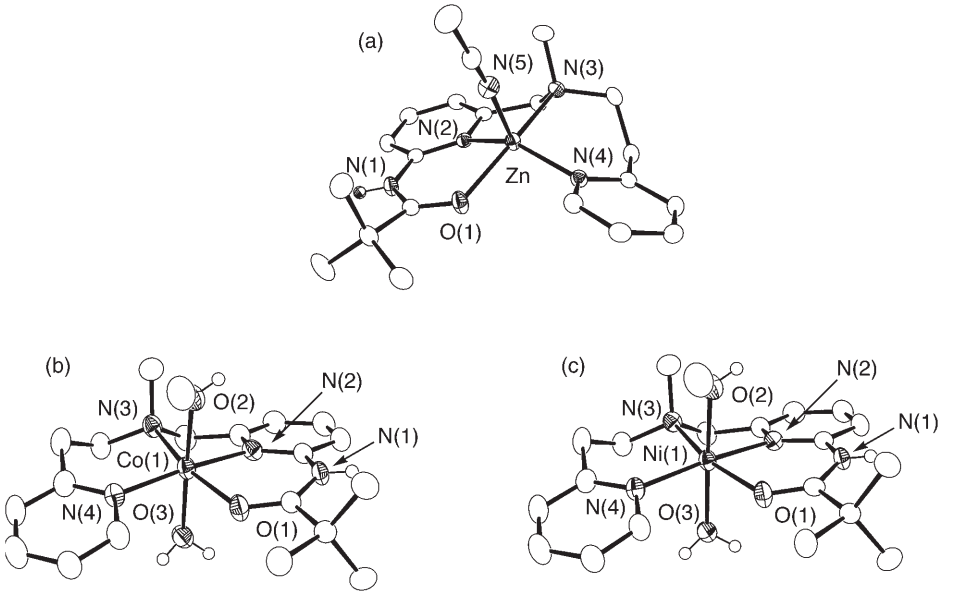

Figure 2. ORTEP drawings of the cationic portions of **1**, **2** · **H$_2$O**, and **3**. All ellipsoids are drawn at the 50% probability level. All hydrogen atoms are omitted from drawings except the amide hydrogen atoms and those present on coordinated solvent molecules.

Table 1. Summary of X-ray data collection and refinement.

	1	**2** · **H$_2$O**	**3**
Empirical formula	$C_{21}H_{29}N_5O_9Cl_2Zn$	$C_{20}H_{30}N_4O_{10}Cl_2Co\text{-}H_20$	$C_{20}H_{32}N_4O_{11}Cl_2Ni$
Formula weight	631.76	634.33	634.11
Crystal system	monoclinic	orthorhombic	orthorhombic
Space group	$P2_{1/c}$	$P2_12_12_1$	$P2_12_12_1$
a (Å)	14.7345(4)	11.7565(2)	11.6628(3)
b (Å)	12.1430(3)	14.6843(5)	14.6786(6)
X (Å)	15.8589(2)	15.8284(5)	15.8882(7)
α (°)	90	90	90
β (°)	113.7095(14)	90	90
γ (°)	90	90	90
V (Å^3)	2597.99(10)	2732.55(14)	2719.96(18)
Z	4	4	4
Density (Calcd) (Mg m^{-3})	1.615	1.542	1.548
Temp (K)	150(1)	150(1)	150(1)
Crystal size (mm^3)	$0.30 \times 0.18 \times 0.10$	$0.23 \times 0.15 \times 0.10$	$0.25 \times 0.23 \times 0.13$
Diffractometer	Nonius KappaCCD	Nonius KappaCCD	Nonius KappaCCD
Abs. coeff. (mm^{-1})	1.211	0.886	0.972
2θ max (°)	54.96	54.94	54.94
Reflections collected	10459	6134	6171
Indep. reflections	5916	6134	6171
Variable parameters	460	473	473
R_1/wR_2[b]	0.0322/0.0718	0.0397/0.0704	0.0386/0.0791
Goodness-of-fit (F^2)	1.042	1.089	1.139
Largest diff. (e Å^{-3})	0.476, −0.421	0.339, −0.328	0.366, −0.313

[a]Radiation used: Mo-Kα ($\lambda = 0.71073$ Å). [b]$R1 = \Sigma \| F_o | - | F_c \| / \Sigma | F_o |$;
$wR2 = [\sum[w(F_o^2 - F_c^2)]/[\sum(F_o^2)^2]]^{1/2}$ where $w = 1/[\sigma^2(F_o^2) + (aP)^2 + bp]$.

Table 2. Selected Bond Distances (Å) and Angles (deg)[a].

1			
Zn(1)–O(1)	2.0765(14)	N(4)–Zn(1)–N(2)	147.31(6)
Zn(1)–N(2)	2.0619(15)	N(4)–Zn(1)–N(5)	98.67(6)
Zn(1)–N(3)	2.1317(16)	N(2)–Zn(1)–N(5)	113.61(6)
Zn(1)–N(4)	2.0352(16)	N(4)–Zn(1)–O(1)	90.59(6)
C(5)–O(1)	1.232(2)	N(2)–Zn(1)–O(1)	84.40(6)
C(5)–N(1)	1.359(2)	N(5)–Zn(1)–O(1)	90.38(6)
N(5)–Zn(1)–N(3)	100.93(6)	N(4)–Zn(1)–N(3)	97.08(6)
O(1)–Zn(1)–N(3)	165.18(6)	N(2)–Zn(1)–N(3)	82.30(6)
2 · H_2O			
Co(1)–O(1)	2.052(2)	O(1)–Co(1)–N(4)	97.19(9)
Co(1)–O(2)	2.120(2)	O(1)–Co(1)–N(2)	84.11(9)
Co(1)–O(3)	2.155(2)	N(4)–Co(1)–N(2)	173.14(10)
Co(1)–N(2)	2.091(2)	O(1)–Co(1)–O(2)	87.26(9)
Co(1)–N(3)	2.127(2)	N(4)–Co(1)–O(2)	93.39(9)
Co(1)–N(4)	2.085(2)	N(2)–Co(1)–O(2)	93.40(9)
C(5)–O(1)	1.236(3)	O(1)–Co(1)–N(3)	165.33(9)
C(5)–N(1)	1.349(4)	N(4)–Co(1)–N(3)	97.48(10)
N(4)–Co(1)–O(3)	86.20(9)	N(2)–Co(1)–O(3)	81.26(9)
N(2)–Co(1)–O(3)	87.08(9)	O(2)–Co(1)–N(3)	92.37(9)
O(2)–Co(1)–O(3)	176.76(9)	O(1)–Co(1)–O(3)	89.60(9)
N(3)–Co(1)–O(3)	90.88(9)		
3			
Ni(1)–O(1)	2.039(2)	O(1)–Ni(1)–N(2)	85.41(9)
Ni(1)–O(2)	2.091(2)	O(1)–Ni(1)–N(4)	94.96(9)
Ni(1)–O(3)	2.113(2)	N(4)–Ni(1)–N(2)	173.53(10)
Ni(1)–N(2)	2.047(3)	O(1)–Ni(1)–N(3)	167.49(9)
Ni(1)–N(3)	2.089(2)	N(2)–Ni(1)–N(3)	82.14(10)
Ni(1)–N(4)	2.062(2)	N(4)–Ni(1)–N(3)	97.54(10)
C(5)–O(1)	1.239(3)	O(1)–Ni(1)–O(2)	87.25(9)
C(5)–N(1)	1.352(4)	N(2)–Ni(1)–O(2)	93.77(10)
N(2)–Ni(1)–O(3)	86.96(10)	N(4)–Ni(1)–O(2)	92.70(9)
N(4)–Ni(1)–O(3)	86.58(9)	N(3)–Ni(1)–O(2)	92.45(10)
N(3)–Ni(1)–O(3)	90.99(10)	O(1)–Ni(1)–O(3)	89.45(9)
O(2)–Ni(1)–O(3)	176.55(10)		

[a]Estimated standard deviations in the last significant figure are given in parentheses.

In a series of X-ray crystallographically characterized Mn(II) halide complexes of mpppa, [(mpppa)Mn(X)($HOCH_3$)]ClO_4 (X = Cl, Br, I), the four donor atoms of the chelate ligand are coordinated such that the halide and solvent are located in *cis* positions [10]. Thus, the nature of the metal ion and/or the exogenous ligands can result in different coordination motifs for the mpppa chelate ligand.

3.1.4. Spectroscopic characterization. When dissolved in CD_3OD, **1** exhibits ^{1}H NMR signals consistent with the features found in the X-ray structure of this complex. The *t*-butyl methyl proton signal is found at 1.51 ppm, downfield of the position of this signal in the free ligand (1.26 ppm in CD_3CN) and similar in chemical shift to that found for *t*-butyl of [(ppbpa)Zn]$(ClO_4)_2$ (1.56 ppm in CD_3CN) [5]. For both complexes, a downfield shift in the position of many of the ligand proton resonances relative to their positions in the free ligand is consistent with the electron withdrawing effect of the zinc center. As expected based on the X-ray structure, the

benzylic protons of mpppa in **1** are diastereotopic, with doublets at 4.24 and 3.95 ppm, respectively.

When dissolved in methanol, the absorption spectrum of **2** contains a *d-d* transition at 500 nm ($\varepsilon = 20\,M^{-1}\,cm^{-1}$). The intensity of this absorption is consistent with the Co(II) center having a coordination number of six in solution [15]. The absorption spectrum of **3** in methanol contains two absorptions at 578 ($\varepsilon = 7\,M^{-1}\,cm^{-1}$) and 850 ($16\,M^{-1}\,cm^{-1}$) nm that can be assigned as *d-d* transitions.

The infrared spectral features of **1**–**3** (in KBr) in the region of ~1700–1600 cm^{-1} range are generally similar and indicative of the presence of an oxygen-coordinated amide moiety. Specifically, whereas the $\nu_{C=O}$ vibration in the free mpppa ligand is found at 1688 cm^{-1}, in these complexes this vibration is found at lower energy (~1660 cm^{-1}) due to enhanced C-O single bond character in the metal-coordinated amide.

3.2. *Amide cleavage reactivity of 1*

3.2.1. Product identification. Heating of **1** with an equimolar amount of $Me_4NOH \cdot 5H_2O$ in methanol for 24 h at 45° C results in amide methanolysis as outlined in scheme 2. Formation of methyl trimethylacetate was indicated by the appearance of a new singlet at 1.17 ppm [5]. The formation of one equivalent of Me_4NClO_4 is proposed based on: (a) the formation of a solid in the reaction mixture upon treatment of **1** with $Me_4NOH \cdot 5H_2O$, and (b) the previous identification and quantification of Me_4NClO_4 as a similarly produced solid in the amide methanolysis reaction of $[(ppbpa)Zn](ClO_4)_2$ [5]. A control reaction indicated that the triflate analog of **1** does not undergo amide methanolysis in the absence of $Me_4NOH \cdot 5H_2O$. In a large scale reaction involving treatment of the triflate analog with $Me_4NOH \cdot 5H_2O$ in methanol, the primary amine ligand product, *N*-((6-amino-2-pyridyl)-*N*-methyl-*N*-(2-pyridylethyl)amine (apmpa), was isolated in 89% yield following treatment of the reaction mixture with aqueous Na_2EDTA to remove the zinc ion. The apmpa product was characterized by ^1H and $^{13}C\{^1H\}$ NMR, an accurate mass measurement, and infrared spectroscopy.

3.2.2. Isolation and characterization of $[(mpppa^-)Zn]ClO_4$ (4). Treatment of **1** with an equimolar amount of $Me_4NOH \cdot 5H_2O$ in acetonitrile/methanol initially results in formation of a deprotonated amide complex, which was isolated and characterized. The combustion analysis of this deprotonted amide complex is consistent with the formulation $[(mpppa^-)Zn]ClO_4$ (**4**) and no coordinated solvent. Infrared analysis of a solid sample of **4** provided additional evidence for the presence of a deprotonated amide. Specifically, the amide carbonyl vibration present in **1** at 1660 cm^{-1} is not present in **4**, and a region of intense vibrations is found centered at ~1450 cm^{-1}. This is consistent with deprotonation of the amide and formation of a resonance-stabilized anion wherein the C–O unit has partial multiple bond character [5].

Analytically pure **4** exhibits temperature and concentration dependent ^1H NMR features. For example, at 338 K and 0.1 M, a single set of broadened ligand resonances

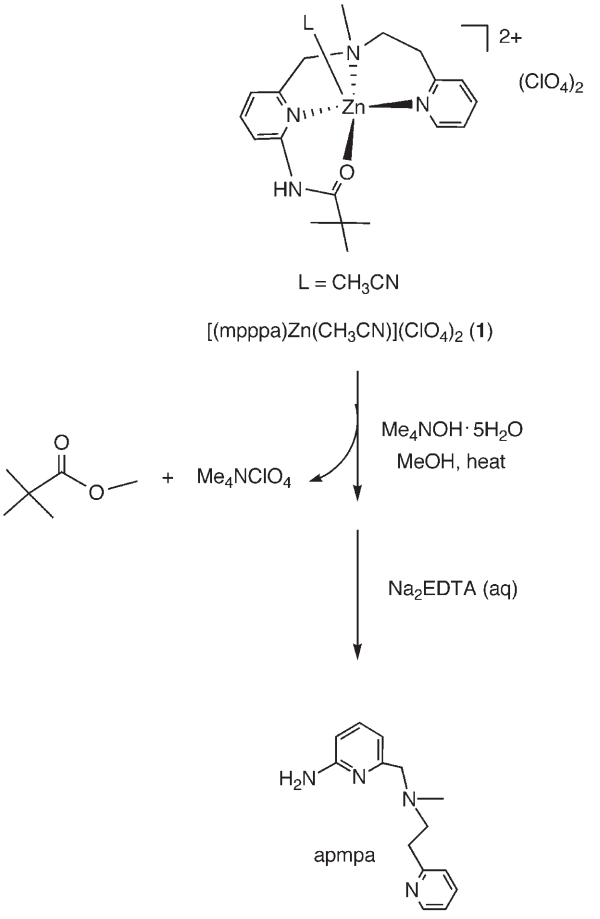

Scheme 2. Amide methanolysis reactivity of **1**.

is present with a *t*-butyl methyl signal at 1.22 ppm and five resonances in the aromatic region, of which three signals each integrate to one hydrogen and two signals each integrate to two hydrogens for a total seven aromatic protons (figure 3(top)). The *t*-butyl methyl signal is ~0.2 ppm upfield of the corresponding signal in **1**. A broad aromatic resonance at ~6.85 ppm (2H) in the spectrum of **4** is upfield of the aromatic resonances exhibited by the parent **1**. These spectral features are consistent with amide deprotonation and delocalization of the anion to the β-positions of the pyridyl ring as described for [(ppbpa$^-$)Zn]ClO_4 [5]. Upon cooling of the 0.1 M solution of **4** to 298 K the *t*-butyl methyl signal broadens and several new broadened resonances appear in the aromatic region (figure 3(bottom)). Increasing the temperature to 338 K again produces the initial spectrum, indicating a reversible process. Cooling of the 0.1 M solution of **4** to 258 K produces a more complicated spectrum containing several overlapping broad resonances in the aromatic and aliphatic regions of the spectrum. The ^{1}H NMR features of a lower concentration solution of **4** in CD_3CN (0.01 M) at 298 K are identical to those shown in figure 3(bottom). We believe that the ^{1}H NMR features of analytically pure **4** are consistent with the presence of an equilibrium

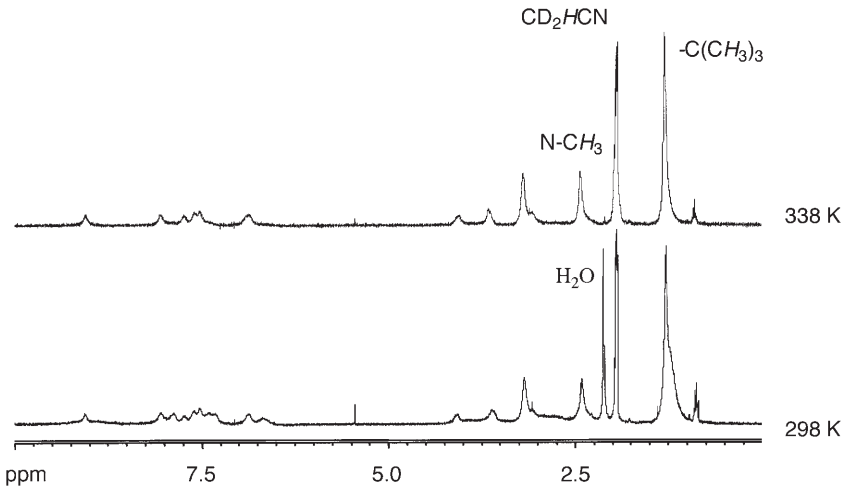

Figure 3. ^{1}H NMR spectra of **4** (0.1 M) at 338 and 298 K.

Table 3. Rate constants for the amide methanolysis reaction of **1** in CD_3OD:CD_3CN[a].

Temperature (K)	$k_{obs}(s^{-1})$
315	$5.1(2) \times 10^{-5}$
325	$1.3(2) \times 10^{-4}$
336	$3.4(3) \times 10^{-4}$
346	$8.0(6) \times 10^{-4}$

[a][**1**] = 0.021 M, [CD_3OD] = 15.4 M.

involving mono- and multinuclear cations. The formation of a multinuclear cation might occur via bridging of a deprotonated amide oxygen atom, which has an available lone pair of electrons. Attempts to obtain a crystalline sample of **4** suitable for X-ray crystallography have thus far been unsuccessful as the complex is quite soluble in acetonitrile, methanol, and diethyl ether. Precipitation of **4** as a white powder is possible by combining a methylene chloride solution of the complex with excess hexane, however a crystalline solid has not been obtained using this method.

3.2.3. NMR kinetic studies of the amide methanolysis reaction of 1. The amide methanolysis reaction which occurs upon treatment of **1** with $Me_4NOH \cdot 5H_2O$ in CD_3OD:CD_3CN, and proceeds via the initial formation of **4**, was monitored by ^{1}H NMR. Rate data were collected by monitoring the loss of the *t*-butyl methyl signal of **4** at a specified temperature. Pseudo-first-order rate constants (k_{obs}) were determined from the slopes of plots of ln[**4**] versus time (table 3). A typical correlation coefficient (R^2) for these plots was $\geq$0.998. A run performed at 63°C using isolated, analytically pure **4** in CD_3OD:CD_3CN (15.4 M) produced a rate constant that is within experimental error of that starting from **1**. This is consistent with **4** being an intermediate generated prior to the rate-determining step of the amide methanolysis reaction.

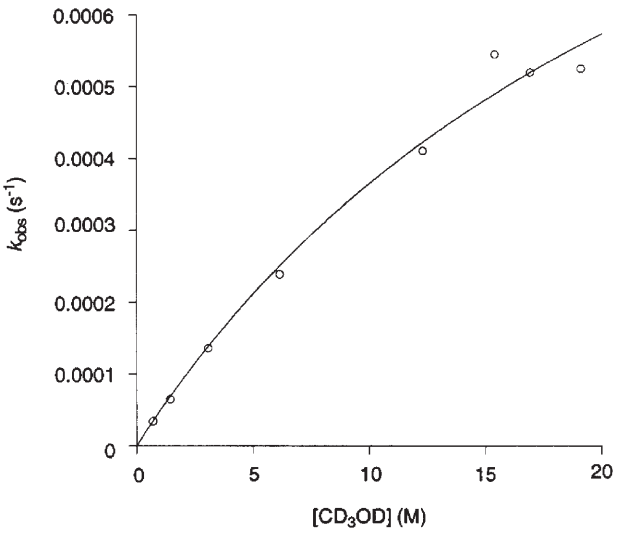

Figure 4. Plot of [CD_3OD] versus k_{obs} for the amide methanolysis reaction of **1** at 336 K. These experiments were performed with [CD_3OD] = 0.71 M-19.1 M in CD_3CN and [**1**] = 0.021 M.

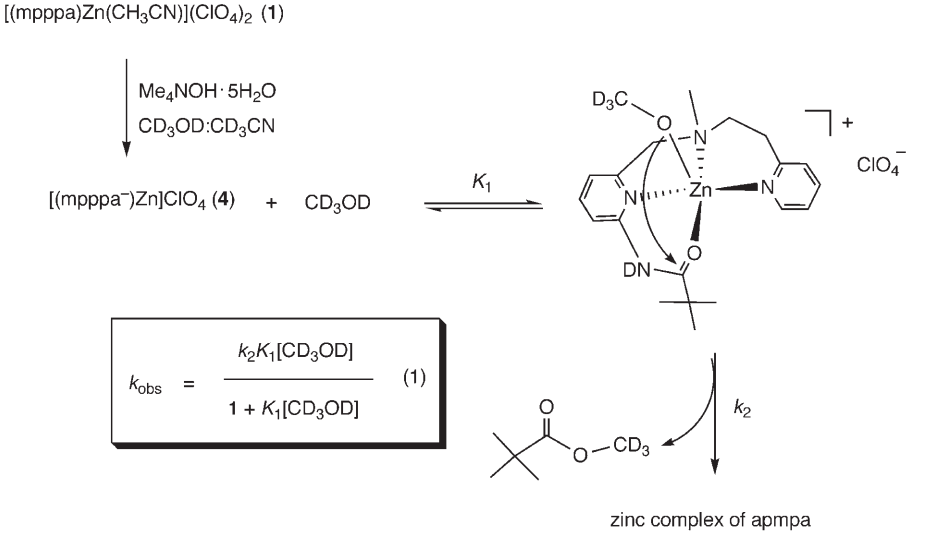

Scheme 3. Proposed mechanism for the amide methanolysis reaction of **1**.

Evaluation of the rate as a function of [CD_3OD] was performed for the range of 0.71–19.1 M. A plot of k_{obs} versus [CD_3OD] is shown in Figure 4. This plot reveals saturation-type behavior in terms of the methanol concentration. Notably, saturation behavior was not evident in the amide methanolysis reaction of [(ppbpa)Zn](ClO_4)$_2$, but was identified for the amide hydrolysis reaction of the same complex [4,5]. As was described for the hydrolysis of [(ppbpa)Zn](ClO_4)$_2$, these data are consistent with a mechanism wherein an equilibrium occurs prior to an irreversible step (Scheme 3). Using equation 1 to fit the data shown in figure 4, values for the equilibrium constant

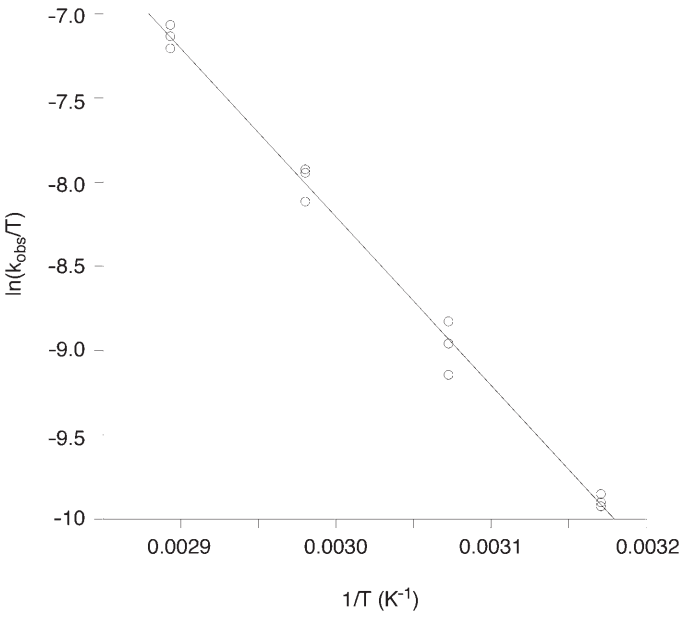

Figure 5. Eyring plot for the amide methanolysis of **1**. Reactions were performed with [**1**] = 0.021 M and [CD_3OD] = 15.4 M in CD_3CN. Rate data were collected as a function of temperature for the range of 315–346 K.

Table 4. Thermodynamic data for the amide methanolysis reaction of **1** and the amide methanalysis and hydrolysis reactions of [(ppbpa)Zn]($C1O_4$)$_2$.

	1 methanolysis	[(ppbpa)Zn](ClO_4)$_2$ methanolysis	[(ppbpa)Zn](ClO_4)$_2$ hydrolysis
$\Delta H^{\ddagger}$(kcal/mol)	19.8(3)	15.0(2)	18.0(5)
$\Delta S^{\ddagger}$ eu	−3.8(1)	−28(1)	−22(2)
$T\Delta S^{\ddagger}$(kcal/mol)[d]	−1.1(3)	−8.3(3)	−6.6(6)
$\Delta G^{\ddagger}$(kcal/mol)[e]	20.9(6)	23.3(5)	24.6(11)

[a]Calculated using pseudo first-order (k_{obs}) values. [b]Ref. 5. [c]Ref. 4. [d]298(1) *K*. [e]Calculated from $\Delta G^{\ddagger} = \Delta H^{\ddagger} - T\Delta S^{\ddagger}$ at 298(1) K.

K (0.037(25)) and k_2 ($1.34(32) \times 10^{-4}\,s^{-1}$) were determined. This value of *K* is approximately six-fold smaller than that found in the amide hydrolysis reaction of [(ppbpa)Zn](ClO_4)$_2$ [4]. Differences in the acidity of water and methanol, and/or the basicity of the deprotonated amide complexes would influence the position of this equilibrium. In regard to the latter, the zinc center in the deprotonated amide complex **4** would be expected to have a higher Lewis acidity than the zinc center in [(ppbpa$^-$)Zn]ClO_4 simply due to the lower overall coordination number of the mpppa$^-$ versus the ppbpa$^-$ ligand. This could influence the thermodynamic stability of **4** with respect to protonation relative to the reaction involving [(ppbpa$^-$)Zn]ClO_4.

Kinetic data for the amide methanolysis reaction of **1** were obtained as a function of temperature for the range of 315–346 K and an Eyring plot was constructed (figure 5). The activation parameters derived from this plot are given in table 4 and are compared to those determined for the amide methanolysis and hydrolysis reactions of

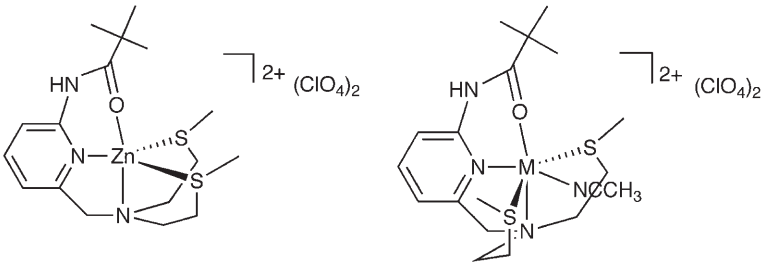

[(bmppa)Zn](ClO$_4$)$_2$ M = Co, [(bmppa)Co(CH$_3$CN)](ClO$_4$)$_2$

M = Ni, [(bmppa)Ni(CH$_3$CN)](ClO$_4$)$_2$

Figure 6. Drawings of bmppa-ligated Zn(II), Co(II), and Ni(II) complexes.

[(ppbpa)Zn](ClO$_4$)$_2$ [4,5]. In the reaction of **1**, a higher $\Delta H^{\ddagger}$ value is offset by a smaller negative $\Delta S^{\ddagger}$ contribution, indicating a less ordered transition state relative to that found in the reactions involving [(ppbpa)Zn](ClO$_4$)$_2$.

Overall, the amide cleavage reactions of **1** and [(ppbpa)Zn](ClO$_4$)$_2$ follow similar mechanistic pathways (scheme 3). Each complex undergoes reaction with $Me_4NOH \cdot 5H_2O$ to produce a deprotonated amide intermediate that subsequently undergoes reaction with solvent (methanol or water) to produce the reactive species for amide cleavage. If the rate-determining steps in these reactions involves the attack of a zinc-bound nucleophile (methoxide or hydroxide) on the amide carbonyl carbon, the differences identified for k_2, $\Delta H^{\ddagger}$, and $\Delta S^{\ddagger}$ for the reaction involving **1** are likely due, at least in part, to differences in the orientation of the coordinated amide moiety relative to the zinc-bound nucleophile. In the reaction involving **1**, a coordinated methoxide ligand may be positioned akin to the acetonitrile donor in **1** (scheme 3). In the amide methanolysis and hydrolysis reactions of [(ppbpa)Zn](ClO$_4$)$_2$ the methoxide-coordinated species is proposed to have a distorted trigonal prismatic geometry wherein the coordinated amide and nucleophile occupy adjacent coordination positions [4,5].

3.3. *Treatment of 2 and 3 with $Me_4NOH \cdot 5H_2O$ in methanol*

Recently, we reported studies of the influence of the nature of the metal center on the amide cleavage reactivity of divalent zinc, cobalt, and nickel complexes (Figure 6) of an amide-appended N_2S_2 ligand (bmppa, *N*,*N*-bis(2-methylthio)ethyl-*N*-((6-pivaloylamido-2-pyridyl)methyl)amine) [16–18]. Upon treatment with $Me_4NOH \cdot 5H_2O$, the zinc, cobalt, and nickel complexes undergo reaction to produce deprotonated amide complexes, which for Co(II) and Ni(II) have been isolated and characterized. Heating of these deprotonated amide complexes at 50°C for five days in methanol results in quantitative amide methanolysis for the zinc complex, ~50% yield of amide methanolysis products for the Co(II) derivative, and no amide methanolysis in the case of the Ni(II) complex. The difference in reactivity identified for these complexes was rationalized on the basis of structural differences in the parent complexes wherein the orientation of the coordinated amide and nucleophile likely differ [18]. With these data in hand, we became interested in evaluating the amide methanolysis reactivity of

mpppa-ligated complexes with metal ions other than Zn(II). Treatment of $[(mpppa)Co(CH_3OH)](ClO_4)_2$ (**2**) with an equimolar amount of $Me_4NOH \cdot 5H_2O$ in methanol followed by heating of the reaction mixture at 50°C for 48 h and removal of the Co(II) ion using aqueous Na_2EDTA, resulted in the isolation of the unaltered mpppa ligand in high yield (>85%). A similar result was found for the Ni(II) analog, $[(mpppa)Ni(CH_3OH)(H_2O)](ClO_4)_2$ (**3**). Notably, the addition of $Me_4NOH{\cdot}5H_2O$ to methanol solutions of **2** and **3** does produce a color change in each case, indicating that a reaction takes place. However, as these reactions did not ultimately result in amide methanolysis, the metal complexes present in these reaction mixtures were not isolated or characterized.

4. Conclusions

The experiments described herein contribute to a growing body of data directed at understanding the mechanistic features of amide cleavage reactions involving divalent metal complexes having a coordinated amide moiety within the chelate ligand structure. The results of this study, when combined with other recent data [4,5,16–18], provide insight into how the unique properties of Zn(II) and its ligand environment influence amide cleavage reactions. Specifically, as Zn(II) has a filled $3d^{10}$ shell, the geometric arrangement of ligands in Zn(II) complexes is determined only by the steric and electronic properties of the ligand [19]. This enables the formation of coordination complexes having somewhat unusual coordination motifs, which appear to be essential for amide cleavage reactivity. For example, in zinc complexes of the ppbpa ligand and analogs, a distorted trigonal prismatic geometry is proposed for the active species for amide methanolysis [4,5,17,18]. For the mpppa-ligated zinc complex described herein, the specific geometry of the complex that undergoes amide methanolysis is not known. However, a common feature of the chemistry of amide-appended chelate ligand complexes examined thus far is that when the zinc center is replaced by an open shell 3*d* metal ion (e.g. Co(II) (d^7) or Ni(II) (d^8)) amide cleavage reactivity is either significantly slower or does not occur. In such complexes, ligand field effects influence the geometry at the metal center, and the lack of amide cleavage reactivity is likely due to a different orientation between the coordinated amide and nucleophile.

Supplementary material

CCDC 648457-648459 contain the supplementary crystallographic data for this paper. This data can be obtained free of change from The Cambridge Crystallographic Data Centre via www.ccdc.cam.ac.uk/data_request/cif.

Acknowledgment

This work was supported by the National Science Foundation (CHE-0094066).

References

[1] S. Yamaguchi, A. Wada, Y. Funahashi, S. Nagatomo, T. Kitagawa, K. Jitsukawa, H. Masuda. *Eur. J. Inorg. Chem.*, 4378 (2003).
[2] K. Jitsukawa, Y. Oka, S. Yamaguchi, H. Masuda. *Inorg. Chem.*, **43**, 8119 (2004).
[3] K. Jisukawa, Y. Oka, H. Einaga, H. Masuda. *Tetrahedron Lett.*, **42**, 3467 (2001).
[4] E. Szajna-Fuller, G.K. Ingle, R.W. Watkins, A.M. Arif, L.M. Berreau. *Inorg. Chem.*, **46**, 2353 (2007).
[5] E. Szajna, M. Makowska-Grzyska, C.C. Wasden, A.M. Arif, L.M. Berreau. *Inorg. Chem.*, **44**, 7595 (2005).
[6] J.C. Mareque-Rivas, E. Salvagni, R. Prabaharan, R.T.M. de Rosales, S. Parsons. *Dalton Trans.*, 172 (2004).
[7] J.C. Mareque-Rivas, E. Salvagni, R.T.M. de Rosales, S. Parsons. *Dalton Trans.*, 3339 (2003).
[8] J.C. Mareque-Rivas, R.T.M. de Rosales, S. Parsons. *Dalton Trans.*, 2156 (2003).
[9] J.C. Mareque-Rivas, E. Salvagni, S. Parsons. *Dalton Trans.*, 4185 (2004).
[10] A.L. Fuller, R.W. Watkins, A.M. Arif, L.M. Berreau. *Inorg. Chim. Acta*, **359**, 1282 (2006).
[11] W.C. Wolsey. *J. Chem. Educ.*, **50**, A335 (1973).
[12] Z. Otwinowski, W. Minor. *Methods Enzymol.*, **276**, 307 (1997).
[13] G. M. Sheldrick, University of Göttingen: Göttingen, Germany, 1997.
[14] A.W. Addison, T.N. Rao, J. Reedijk, J. van Rijn, G.C. Verschoor. *Dalton Trans.*, 1349 (1984).
[15] D.R. McMillin. In *Physical Methods in Bioinorganic Chemistry*, L. Que, Jr (Eds), p. 45, University Science Books, Sausalito, CA (2000).
[16] L.M. Berreau, M.M. Makowska-Grzyska, A.M. Arif. *Inorg. Chem.*, **39**, 4390 (2000).
[17] G.K. Ingle, M.M. Makowska-Grzyska, E. Szajna-Fuller, I. Sen, J.C. Price, A.M. Arif, L.M. Berreau. *Inorg. Chem.*, **46**, 1471 (2007).
[18] G.K. Ingle, M.M. Makowska-Grzyska, A.M. Arif, L.M. Berreau, *Eur. J. Inorg. Chem.*, 5262 (2007).
[19] G. Parkin. *Chem. Rev*, **104**, 699 (2004).